LABORATORI NAZIONALI DI FRASCATI
SIS – Pubblicazioni

LNF–99/008 (P)
16 Marzo 1999

Bragg reflecting zones from x-ray diffractors with different surface profiles

A. Marcelli
INFN - Laboratori Nazionali di Frascati, P.O. Box 13, 00044 Frascati, Italy

A.V. Soldatov, M.I. Mazuritsky, V.L. Lyashenko and E.M. Latush
Faculty of Physics, Rostov University, Sorge 5, Rostov-na-Donu, 344090 Russia

Abstract

The knowledge of the area and the shape of the crystal surface that reflects x-rays within a fixed range of angles and at a desired spectral resolution is determinant to evaluate the performances of a x-ray diffractor. In the present study a new mathematical approach that allows the calculation of the Bragg reflection zones has been developed and applied to spherical, toroidal and ellipsoidal diffractors. The reflecting areas of ellipsoidal and toroidal diffractors have been calculated as a function of the surface curvature parameters. Maps of the diffraction areas for different Bragg angles and bandwidths will be presented for each diffractors. The limitations of the existing methods, based on the Tailor series expansion, for the theoretical analysis of Bragg reflection zones are also discussed.

PACS: 07.85.-m
Key words: X-ray instrumentation

Submitted to J. Synch. Rad.

1 - INTRODUCTION

Perfect crystals like quartz, Si, Ge, as well as mosaic crystals like mica or graphite are typically used to diffract x-rays. Standard focusing x-ray spectroscopic devices[1,2] use the reflection of the intrinsic x-ray radiation by the atomic planes of these crystals under the Bragg condition:

$$n\lambda = 2d \sin\theta \qquad (1)$$

where n is an integer representing the order of the reflection, λ is the wavelength of the incident radiation, θ is the angle of glancing of the incident x-ray beam (the complement of the optical angle of incidence) and d is the lattice plane spacing. Almost in all focusing design the curvature of the atomic planes is the same of the crystal surface curvature. Therefore we will assume in the next that the diffracting crystalline planes are parallel to the crystal surface.

For a diffractor device working in the Bragg geometry, two conditions have to be fulfilled to observe the reflection of the x-rays:

1. for each reflecting point the incident and the reflecting angles must be equal;
2. for a definite interval of wavelength $\lambda - \Delta\lambda \leq \lambda \leq \lambda + \Delta\lambda$, the glancing incidence θ angle, satisfying the Bragg's equation, lays in the range $\theta - \Delta\theta \leq \theta \leq \theta + \Delta\theta$, and the value of $\Delta\theta$ is determined by the equation

$$\Delta\theta = (\Delta\lambda/\lambda)\, tg\,\theta \qquad (2)$$

For an ideal device, an increase of $\Delta\theta$ means a greater effective reflection area and therefore a larger aperture of the diffractor. However, for bent crystal devices the two above mentioned conditions imply that the radiation is diffracted and focused only by a small area of the bent crystalline surface. As a consequence, although the x-ray reflection intensity should increase with $\Delta\theta$, on the another hand a widening of the illuminated area, does not produce an increase of the flux because of the decrease of the spectral resolution $\Delta\lambda / \lambda$ (see Eq. 2). In fact, in a practical device one needs to find a compromise between the highest possible spectral resolution associated to a small reflecting surface and a large diffractor aperture that usually is possible only selecting a low spectral resolution. Actually, for a bent device, a real increase of the aperture should be obtained only increasing the effective reflecting area of a diffractor without changing resolution or $\Delta\theta$. To demonstrate the possibility to achieve this challenging result, approximate analytical calculations of the geometrical and spectral parameters of the reflecting areas of bent crystal diffractors, using different methods, have been already performed[3-9]. The results were obtained using an analytical function of the scalar product of two vectors, both starting from the point $\boldsymbol{P}$ (XYZ) and laying on the diffractor surface: the normal vector $\boldsymbol{n}$ and the vector $\boldsymbol{PS}$. Here the point $\boldsymbol{S}$ indicates the source of the x-ray radiation. Within this framework, a function

$$\Phi\,(X,Y,Z) = (\mathbf{n} \cdot \mathbf{PS})/|\mathbf{n}||\mathbf{PS}| = \sin(\theta \pm \Delta\theta) \qquad (3)$$

may be defined, and an approximate solution $\Delta\theta$ can be obtained using the Tailor series expansion:

$$\Delta\theta = AX^2 + BX^3 + CZ^2 + DXZ^2 \qquad (4)$$

where *A, B, C* and *D* are the coefficients of the series [3-8]. In addition,

$$\boldsymbol{Y}=\sqrt{1-X^2-Z^2} \tag{5}$$

and *X, Y* and *Z* are the relative coordinates, in the units of the curvature radius, of the bent crystal in the X,Y plane. Here and within all the manuscript we consider the same coordinate grid used in ref.[3-9], where focusing circle is set in the XY plane and (0,0,0) are the coordinates of the center of the focusing circle.
Here we define a spherical crystal surface as:

$$\Delta\theta = 1/2\ (X^2\ cotg\,\theta + X^3\ cotg^2\theta + XZ^2\ cotg^2\theta) \tag{6}$$

so that for glancing angle θ>45° (i.e., cot (θ)<1) it is possible to calculate with accuracy the shape of the reflection zone. On the contrary, when θ<45° the approximation of Eq. 6 introduces significant distortions to the shape of the Bragg reflection area. We developed a different scheme of the numerical calculation of the diffractor reflecting area based on the Monte-Carlo method and applied it to different reflecting surfaces: spherical, ellipsoidal and toroidal. Aims of the present work are:

i) to define the limitation of this approach and compare it with the previous analytical methods[3-8] and,
ii) the analysis of the Bragg reflection region of a bent crystal as a function of the incidence angles and the spectral resolution.

2 -THEORETICAL SCHEME

We may start considering an elliptical profile, defined by the equation of an ellipsoid produced by the circle in the XY plane:

$$X^2 + Y^2 + (a/b)^2\ Z^2 = 1 \tag{7}$$

where *a* and *b* are respectively the major and minor semi-axes. When *a=b* the surface become spherical, while the equation for a tore with a circle of radius *a* in the *XY* plane, having the center of the circle with radius *b* around the *Z* axis, is:

$$X^2 + Y^2 = \left(\frac{a}{a+b} + \sqrt{\left(\frac{b}{a+b}\right)^2 - z^2} \right)^2 \tag{8}$$

In equations (7) and (8) ***X***, ***Y*** and ***Z*** are the relative coordinates in the units of the parameter ***a***. We need to define also the vector ***n***, normal to the surface of the diffractor, that point to *P(XYZ)* as

$$\boldsymbol{n} = -\mathbf{X}\boldsymbol{i} - \mathbf{Y}\boldsymbol{j} - \beta\mathbf{Z}\boldsymbol{k} \tag{9}$$

and the vector ***PS*** that can be written as

$$\boldsymbol{PS} = (\cos\theta\sin\theta - \mathbf{X})\ \boldsymbol{i} + (\cos^2\theta - \mathbf{Y})\ \boldsymbol{j} - \mathbf{Z}\ \boldsymbol{k} \tag{10}$$

Sometimes for an ellipsoid is better introduce two equivalent parameters:

$$\alpha=\mathbf{b/a}\ ,\ \beta=1/\alpha^2 \tag{11}$$

useful to describe also a toroidal surface if we change their definitions to

$$\alpha=\frac{b}{a+b},\quad \beta=\frac{(1-\alpha)+\sqrt{\alpha^2-Z^2}}{\sqrt{\alpha^2-Z^2}} \tag{12}$$

Actually, with these two parameters we may describe both surfaces with only one equation

$$Y=\sqrt{\alpha^2\beta^N-X^2-\beta^N Z^2}. \tag{13}$$

where N=1 for the ellipsoid surface and N=2 for the toroidal one. After some algebraic transformations, one may obtain the function Φ(X,Y,Z), that describes the set of the points (X,Y,Z) belonging to the reflecting area of the crystal. When the glancing angle of the x-ray radiation, respect to the crystalline planes, is $\theta \pm \Delta\theta$, the condition that determines the surface of the reflecting zone is:

$$\sin(\theta-\Delta\theta) \le \Phi(X,Y,Z) \le \sin(\theta+\Delta\theta) \tag{14}$$

We will discuss in the next the effects induced by the change of the diffractor parameters within the following limits:

$$0° \le \theta \le 90°;\ 10^{-5} \le \Delta\lambda/\lambda \le 10^{-3};\ |Z|\le 0.2,\ |X|\le 0.2 \tag{15}$$

that correspond respectively to the glancing angle, the resolution and the dimensions of the crystal. Indeed, |**X**| and |**Z**| are the normalized coordinates, i.e., |**X**|=X/(2R) and |**Z**| =Z/(2R) where R is the Rowland circle radius.

3 - DISCUSSION

The comparison between the calculations of the reflecting zones of a spherical crystal diffractor, obtained with the approximate formula discussed in Ref. 3-8 and the expression described above are shown in Fig. 1 and 2.

The approximate expression is a series where each term contains the $\cot\theta$ function. Actually, this function controls the decrease of each contribution for angles θ >45°. As clearly shown in Fig. 1, θ =60° both at $\Delta\theta$ =10^{-4} and $\Delta\theta$ =10^{-5} the shapes obtained by the two methods are almost equivalent. On the contrary when $\cot\theta > 1$, for example at θ =30° deviations in the calculated shape of reflecting zones can be clearly detected. These last also increase with the resolution as demonstrated by the comparison between the data calculated at $\Delta\theta$ =10^{-5} and $\Delta\theta$ =10^{-4} in Fig. 2.

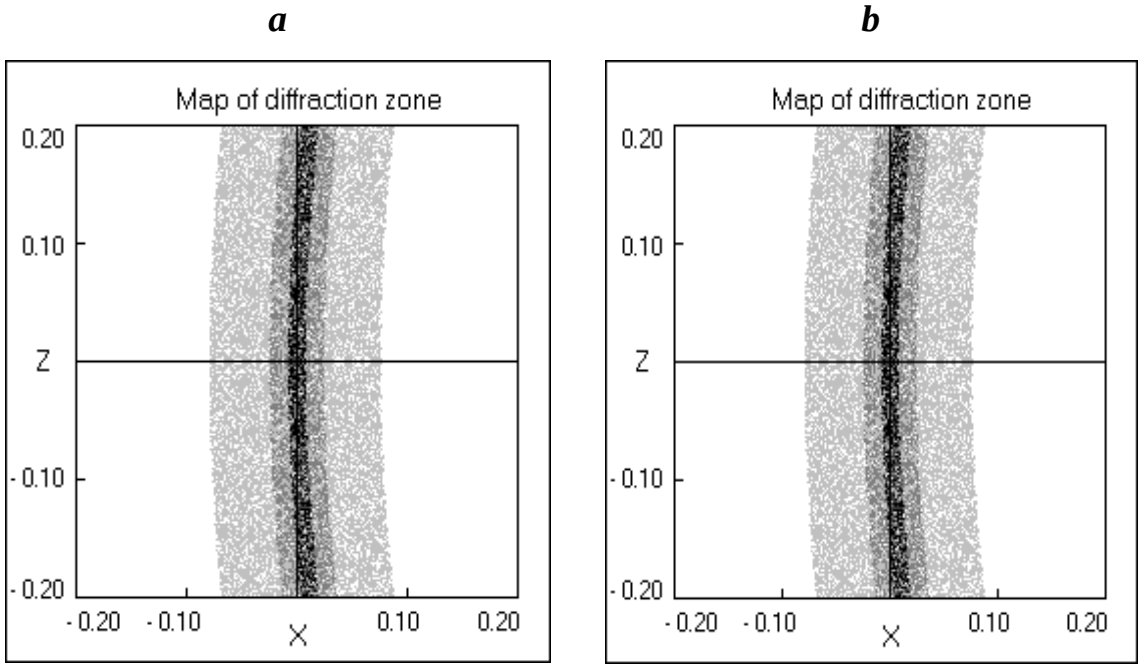

FIG. 1 Bragg reflecting zone (θ =60°) of spherical crystal diffractor using the exact (panel *a*) and the approximate (panel *b*) formula. The data refer to different resolutions, i.e., $\Delta\theta$ =10^{-5} (black); 10^{-4} (dark grey); 10^{-5} (light grey) and clearly show that the Bragg reflection area increases lowering of the resolution.

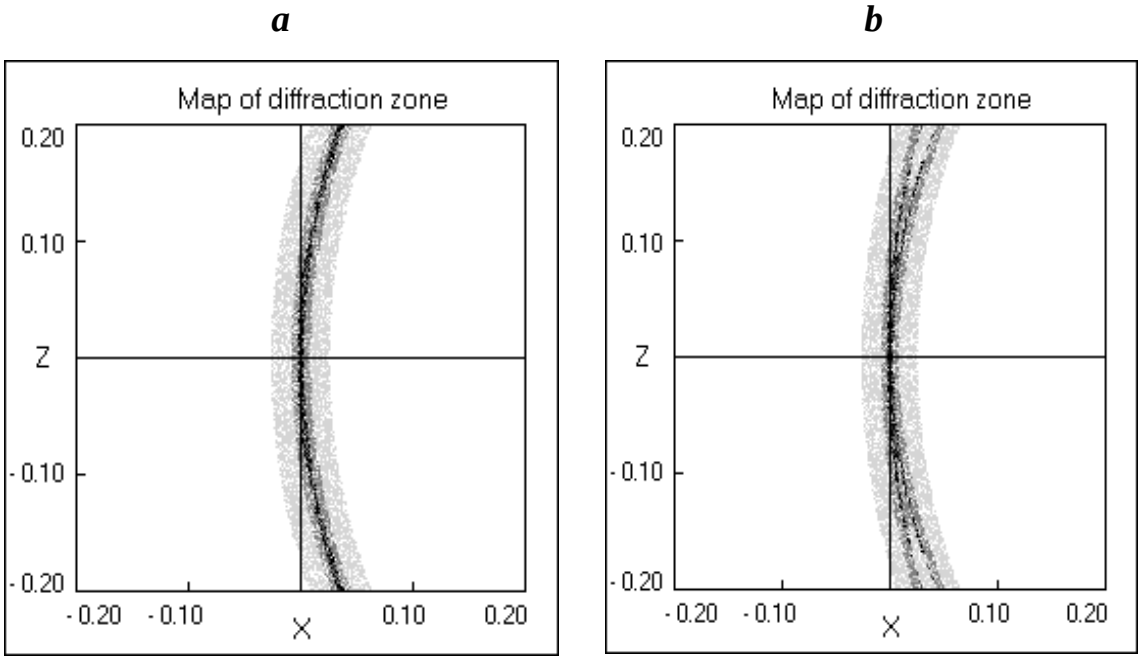

FIG. 2 Bragg reflecting zone (θ =30°) of spherical crystal diffractor using exact (panel *a*) and approximate (panel *b*) formula. The data refer to different resolutions, i.e., $\Delta\theta$ =10^{-5} (black); 10^{-4} (dark grey); 10^{-5} (light grey) and clearly show that the Bragg reflection area increases lowering the resolution.

In Fig. 3 and 4 we present the Bragg reflecting area for ellipsoidal and toroidal diffractors as a function of the ratio of the surface curvature radii, both in the vertical (XZ) plane and in focusing (XY) plane. For each profile we report three curves, corresponding to the Bragg angles of 30°, 45° and 60°. All the curves in Fig. 3 and 4 exhibit two maxima. The maximum *C* corresponds to the set of parameters when ellipse and tore become a sphere, namely for the ellipse having $a=b$ (Fig. 3) and for the tore with $a<<b$ in Fig. 4. For the ellipsoidal diffractors, shown in Fig. 3, the maxima B_1, B_2 and B_3 corresponds to the condition $b=a \sin(\theta)$, where *b* is the distance from the source S to the diffractor center (0,*a*,0). For this maximum the reflecting area at all angles (θ =30°, 45° and 60°) is approximately equal to the effective area of the spherical crystal.

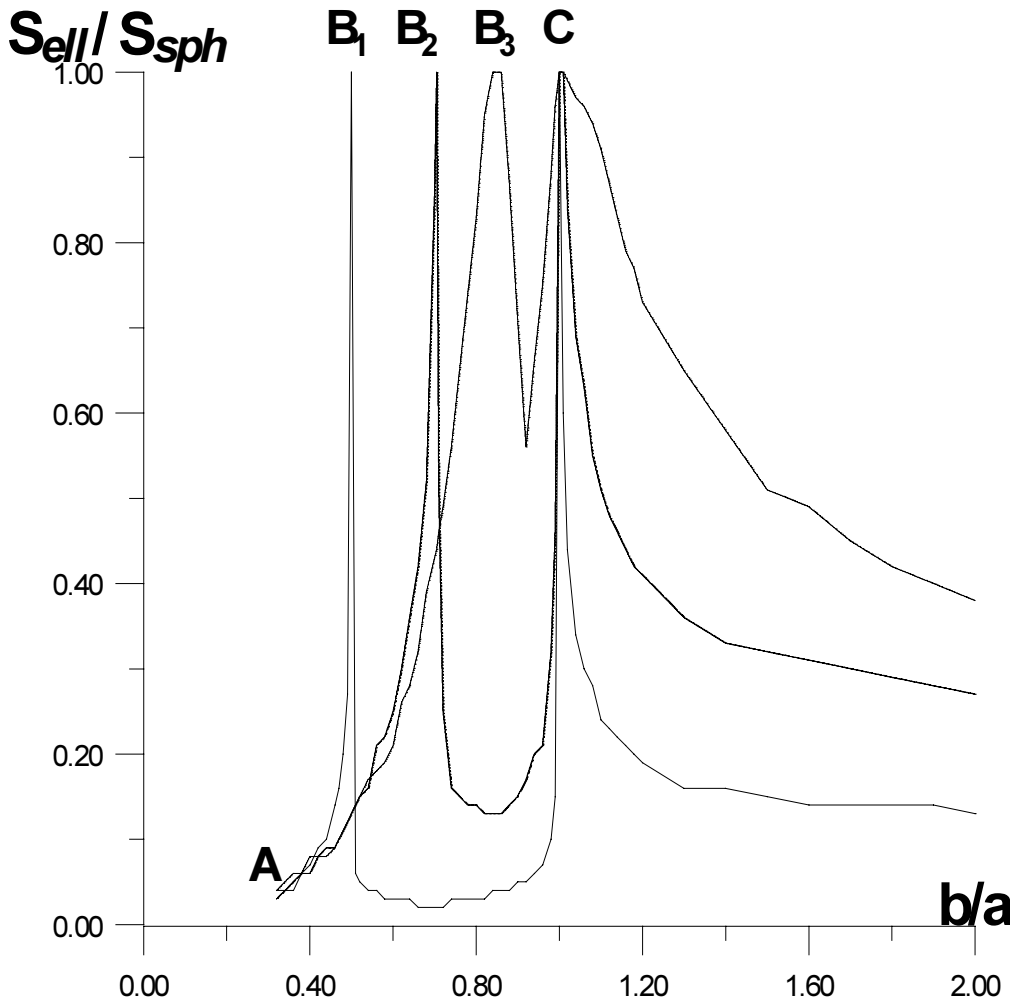

FIG. 3 Dimension of the reflecting zone ($\Delta\theta$ =10^{-4}) of an ellipsoidal diffractor normalized to the area of a spherical step, as a function of the curvatures parameters. S_{ell} - ellipsoid area; S_{sph} - spherical area; a - radius of diffractor curvature in XY plane; b - radius of diffractor curvature in YZ plane. The three curves plotted correspond to the glancing angle: θ =30° (solid); θ =45° (dot) and θ =60° (dot-dashed).

In Fig. 5 we show a few examples of the possible shapes of the reflecting surfaces of an ellipsoidal diffractor working at the Bragg angle of θ =45° and at a resolution of $\Delta\theta$ =10^{-4}. The panel 1 and 2 of Fig. 5 correspond to the area associated to the geometrical conditions of the diffractor characterized by a set between the points A and B_2 in Fig. 3. The Bragg reflecting zone for B_2 is shown in panel 3. If we consider the range between B_2 and C one may obtain results reported in the panels 4 and 5. The reflecting zone for the C point is shown in panel 6, while when b/a>1, i.e., for the range after the point C of Fig. 3, the zone shapes are presented in panels 7 and 8 of Fig. 5.

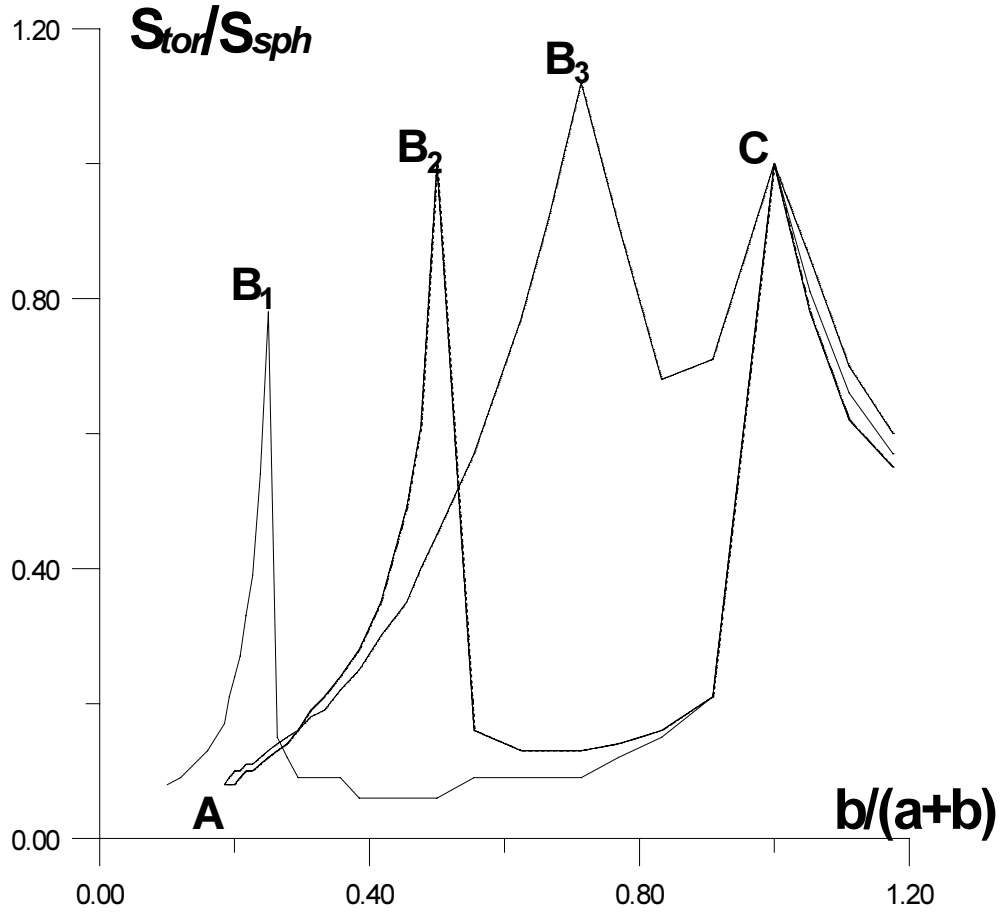

FIG. 4 – Dimension of the reflecting zone ($\Delta\theta$ =10^{-4}) of a toroidal diffractor normalized to the area of a spherical step, as function of curvatures parameters. S_{tor} - toroidal area; S_{sph} - spherical area; $a+b$ - radius of diffractor curvature in XY plane; b - radius of diffractor curvature in YZ plane. The three curves plotted correspond to the glancing angle: θ =30° (solid); θ =45° (dot); θ =60° (dot-dashed).

In the case of a toroidal surface, the radius of the diffractor curvature in the focusing plane is $(a + b)$. The positions of the B maxima correspond to the value of the curvature radius in the *YZ* plane, i.e., $b= (a + b) \sin^2(\theta)$ or in other words, the distance from the center of crystal to the intersection of the normal to S and the OY axis. Figure 4 shows that for angles greater then 45° a toroidal diffractor with parameters a and b in the region of the maximum B_3 is more effective then a spherical one. For this device, we compare in Fig. 6 the shapes of the reflecting zones at the Bragg angle of θ =45° and assuming a resolution of $\Delta\theta$ =10^{-4}.

1

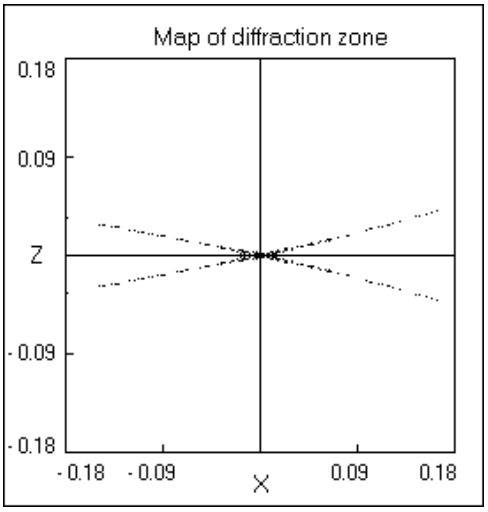
Map of diffraction zone
0.18
0.09
Z
- 0.09
- 0.18
- 0.18
- 0.09
0.09
0.18
X

2

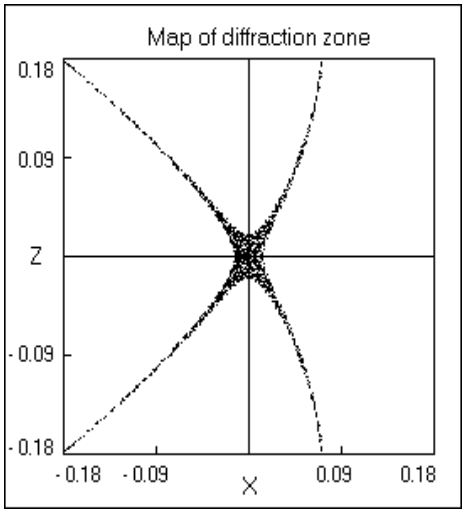
Map of diffraction zone
0.18
0.09
Z
- 0.09
- 0.18
- 0.18
- 0.09
0.09
0.18
X

3

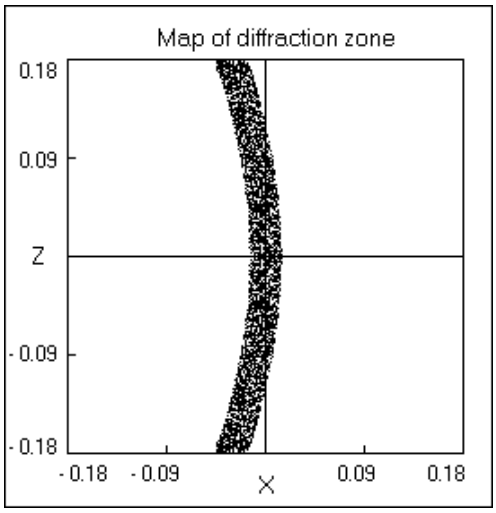
Map of diffraction zone
0.18
0.09
Z
- 0.09
- 0.18
- 0.18
- 0.09
0.09
0.18
X

4

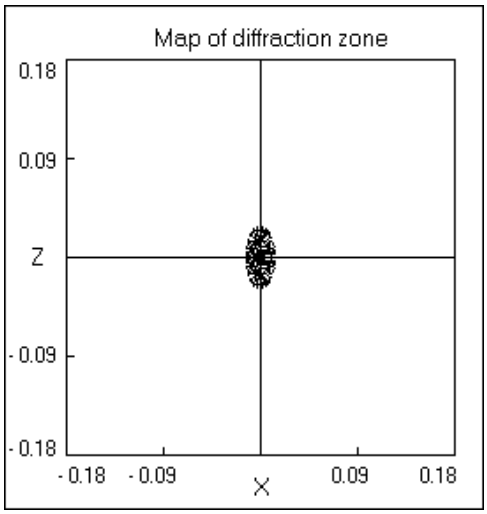
Map of diffraction zone
0.18
0.09
Z
- 0.09
- 0.18
- 0.18
- 0.09
0.09
0.18
X

5

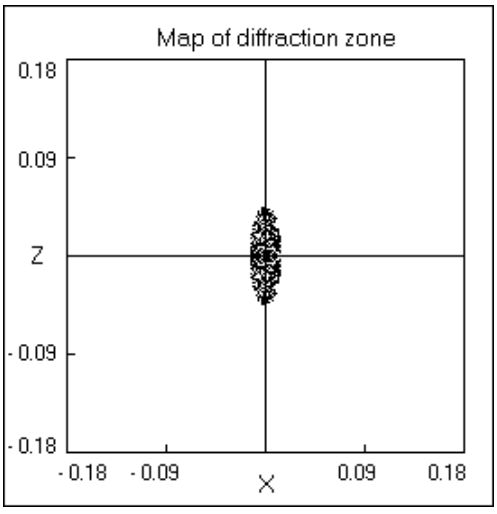
Map of diffraction zone
0.18
0.09
Z
- 0.09
- 0.18
- 0.18
- 0.09
0.09
0.18
X

6

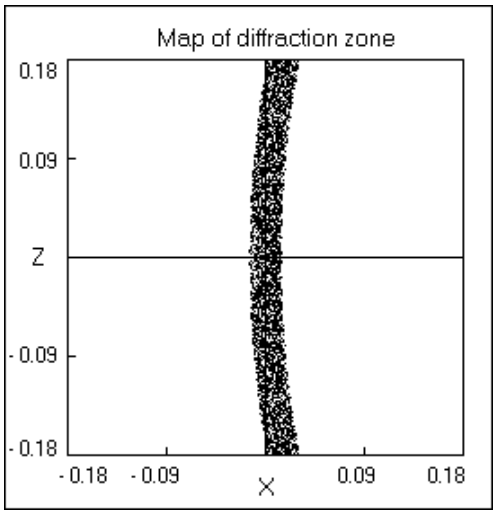
Map of diffraction zone
0.18
0.09
Z
- 0.09
- 0.18
- 0.18
- 0.09
0.09
0.18
X

7 **8**

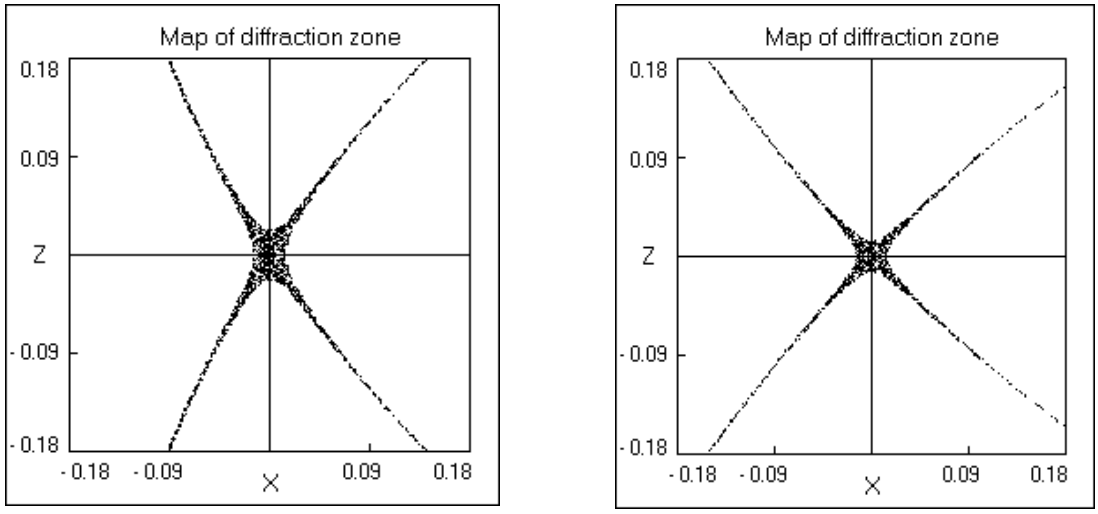

FIG. 5 – Ellipsoidal reflecting zones for an ellipsoidal diffractor at θ =45° and $\Delta\theta$ =10^{-4}. The set of parameters associated to the different panels are: a=1 for all, then from panel 1 to 8 respectively: b=0.4; 0.65; 0.707; 0.8; 0.95; 1; 1.2; 1.6.

The panels 1 and 2 of Fig. 6 show the zone shape of a diffractor characterized by a generic set between the points A to B_2 of the Fig. 4. The panel 3 of figure 6 corresponds to B_2 in Fig. 4, while the panels 4 and 5 of Fig. 6 report Bragg reflecting area in the range between maxima B_2 and C of Fig. 4. The diffracting zone illustrated in the panel 6 corresponds to point C (quasi-spherical case) of Fig. 4 and the panels 7 and 8 present the results for b larger then $a+b$, i.e. for the convex tore geometry. The results reported in Fig. 5 and 6 are particularly stimulating. Indeed, if we now reconsider the ellipsoidal geometry, looking with more care to panels 3 and 6 of Fig. 5, we may observe that the orientation of the two zones is opposite. This behavior demonstrate that, at least in principle, it is possible to design a diffractor with a reflecting zone almost close to the rectangular shape. This condition should be very favorable to maximize the reflecting area of any device, in particular that based on the stepped geometry. Because, as suggested in Ref. 10, it is very important also to consider the vertical size of the diffraction zone in the design of a high throughput stepped diffractor, to maximize the reflected beam, it is important to choose a geometrical set of parameters of the reflecting crystalline planes (like $\boldsymbol{a}$ and $\boldsymbol{b}$) suitable to get a reflection zone close to the rectangular shape. Of course, the condition of a rectangular shape for each step of a multi-stepped diffracting crystal optimize the throughput at constant (and high) resolution.

1

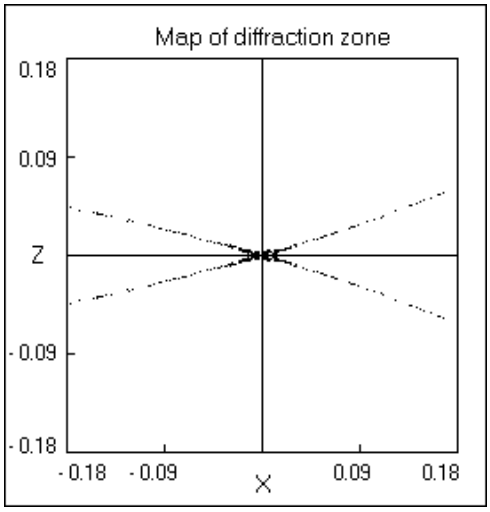
Map of diffraction zone
0.18
0.09
Z
- 0.09
- 0.18
- 0.18
- 0.09
0.09
0.18
X

2

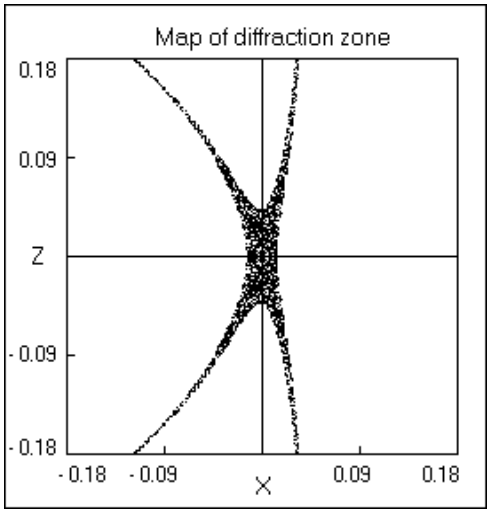
Map of diffraction zone
0.18
0.09
Z
- 0.09
- 0.18
- 0.18
- 0.09
0.09
0.18
X

3

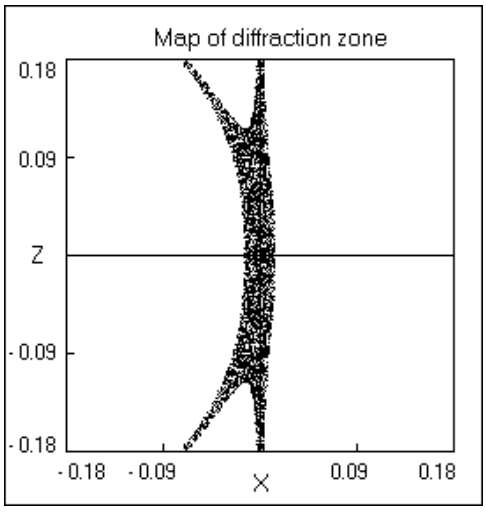
Map of diffraction zone
0.18
0.09
Z
- 0.09
- 0.18
- 0.18
- 0.09
0.09
0.18
X

4

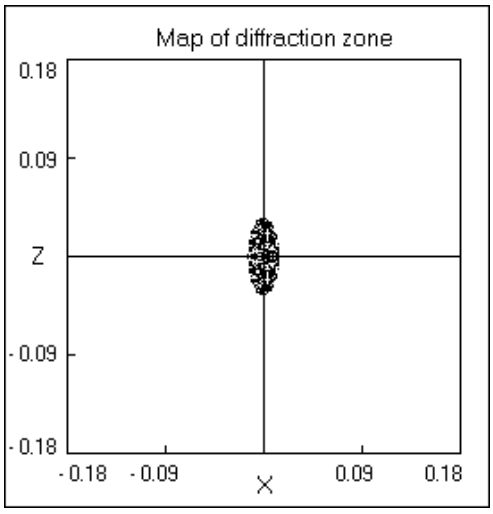
Map of diffraction zone
0.18
0.09
Z
- 0.09
- 0.18
- 0.18
- 0.09
0.09
0.18
X

5

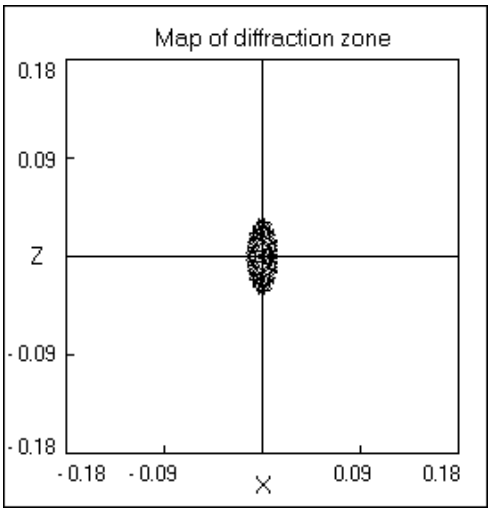
Map of diffraction zone
0.18
0.09
Z
- 0.09
- 0.18
- 0.18
- 0.09
0.09
0.18
X

6

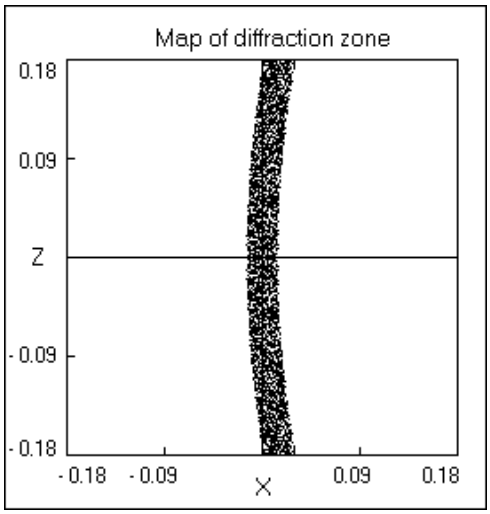
Map of diffraction zone
0.18
0.09
Z
- 0.09
- 0.18
- 0.18
- 0.09
0.09
0.18
X

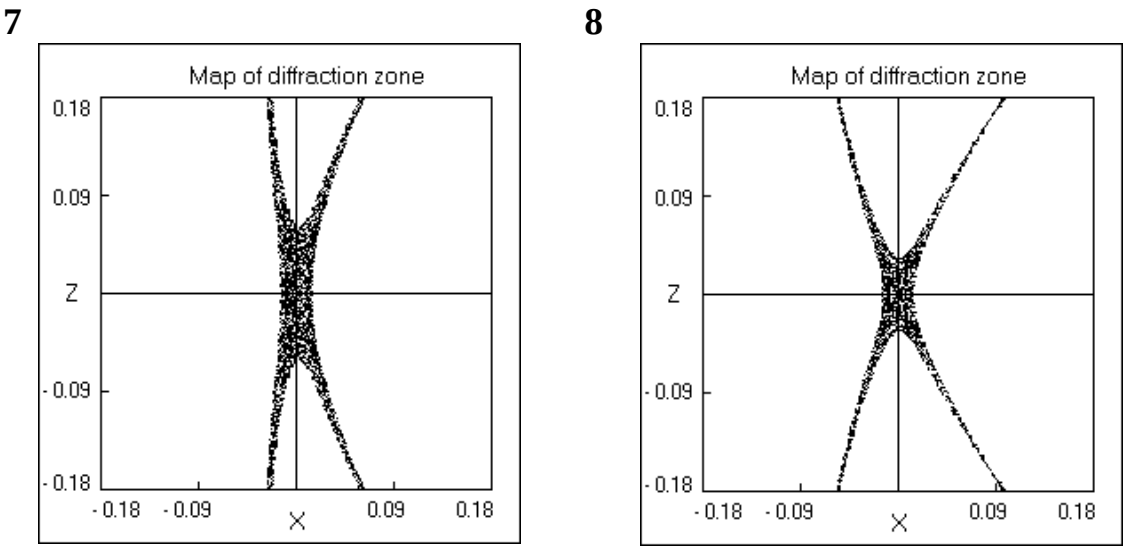

FIG. 6 Toroidal reflecting zones for a toroidal diffractor at θ =45° and $\Delta\theta$ =10^{-4}. The set of parameters associated to the different panels are: (a+b)=1 for all, then from panel 1 to 8 respectively: b=0.2; 0.48; 0.5; 0.56; 0.8; 1; 1.05; 1.18.

The trend observed in the different regions of both ellipsoidal and toroidal diffractors suggest that the calculation of the shape of the reflecting surface may be determinant to design new kind of diffractors such as those necessary to exploit the possibility offered by the new brilliant synchrotron radiation sources. In particular, it appears feasible the design of new diffractors to improve all the devices working in the backscattering geometry now applied to obtain high and ultrahigh resolution i.e., in the meV range[11)].

In particular the design of single or multi-stepped devices will make benefit from this method not only to optimize the performances but also to take advantage of the large flexibility that they offer. Indeed, because a bent crystals in the Rowland circle geometry have been considered only for point to point focusing or point to line focusing, the achievement of a very regular diffractor footprint address also the possibility to work in a non-focusing position. Indeed, in this geometry, working in a position before or after the focus we have, in a definite x-ray bandwidth and with negligible aberration contributions, a regular and homogeneous illuminated area. This unique opportunity will certainly open exciting applications well beyond the standard spectroscopic methods.

In conclusion, a novel approach for a careful, almost exact determination of the Bragg reflection area has been developed and applied to spherical, toroidal and ellipsoidal diffractors. Significant discrepancies of the approximate approach related to the reflecting area of Bragg diffractors have been found and evaluated for Bragg angles less than 45°.

REFERENCES

1. A.G. Michette, Optical System for Soft X-ray, New York and London (1986).
2. A.K. Freund, X-ray Optics, ESRF, Grenoble, (1987).
3. D.B. Wittry and S. Sun, X-ray optics of doubly curved diffractors, J. Appl. Phys.**71**, 546-568, (1992).
4. D.B. Wittry and S. Sun, X-ray optics of doubly curved diffractors, J. Appl. Phys. **67**, 1633-1638, (1990).
5. D.B. Wittry and S. Sun, Focusing properties of curved x-ray diffractors, J. Appl. Phys. **68**, 387-391, (1990).
6. D.B. Wittry and S. Sun, Properties of curved x-ray diffractors with stepped surfaces, J. Appl. Phys. **69**, 3886-3892,(1991).
7. D.B. Wittry and W.Z. Chang, Evaluation of crystal diffractor parameters for curved diffractors, J. Appl. Phys. **72**, 3440-3446,(1992).
8. D.B. Wittry and R.Y. Li, Properties of fixed-position Bragg diffractors for parallel detection x-ray spectra, Rev. Sci. Instrum. **64**, 2195-2200, (1993).
9. D.B. Wittry and W.Z. Chang, Evaluation of crystal diffractors parameters for curved diffractors, J. Appl. Phys. **73**, 601-607, (1993).
10. Marcelli, A. Soldatov and M. Mazuritsky, Pseudo-Spherical Stepped Diffractor Constructed Under Constant Step Width Conditions (Multi-Stepped Monochromator), European Patent No. 97830282.6-2208 (11.06.97).
11. Masciovecchio, U. Bergman, M. Krisch, G. Ruocco, F. Sette and R. Verbeni, A perfect crystal X-ray analyzer with meV energy resolution, Nucl. Instrum. & Meth. **B 111**, 181-186, (1996).